Photocurrents in GaN-based HEMTs: Theoretical model and experimental results

View Online   Export Citation   CrossMark

X. Zheng, (iD) S. Feng,[a] X. Li, Y. Zhang, (iD) and K. Bai

AFFILIATIONS

College of Microelectronics, Beijing University of Technology, Chaoyang, Beijing 100024, China

[a] Author to whom correspondence should be addressed: shwfeng@bjut.edu.cn

ABSTRACT

An experimentally validated model for persistent photocurrents (PPC) in GaN HEMTs has been presented, which can explain both the build-up and decay course. Compared to the popular stretched exponential fit, it employed parameters with a clear physical meaning and could give numerical solutions to predict and support the experimental results. In particular, the effect of the electric field on the photocurrents was found to be closely linked to the probability of the electron-hole recombination used in this model, which provides a way to study the influence of the electric field on PPC. This experimentally verified model with clear and meaningful parameters could be used to better understand the PPC in GaN-based HEMTs.

Published under license by AIP Publishing. https://doi.org/10.1063/1.5128825

In spite of the impressive progress in GaN-based devices, various defects and resultant effects still limit their performance.[1–3] Persistent photocurrents (PPCs) are an increase in the current, upon illumination by light, which persist for a long time even after removing the exciting light, thus hindering the quick recovery of the initial unperturbed state.[4,5] A stretched exponential function, $I(t) = I(0)\exp((-t/\tau)^\beta)$, was employed to explain the PPC decay in most research,[6,7] where $I(0)$ stands for the steady-state current level under the exciting light, τ stands for the time constant of the decay curve, and β stands for the decay exponent. However, this model has a common problem that the physical meaning of β is unclear. In addition, its various values range from 0.1 to 0.28,[8] from 0.46 to 0.79,[9] from 0.7 to 0.8,[10] and from 0.4 to 1,[6] actually leading to a variety of curves, and make it hard to build a physical model. The stretched exponential fit considers fitting the shape of the measured curve rather than the physical essence. In fact, Mitrofanov and Manfra showed that the results deviating from exponentials may be affected by several separate trap levels.[11] Joh and del Alamo suggested that a broad-trap-energy distribution may also result in the deviation from pure exponentials.[12] Although this may provide some possible explanations for the physical meaning of β, it still cannot explain the nonmonotonous PPC build-up and decay course, that is, negative photocurrent (NPC), that sometimes the current increases above the steady exciting current during the build-up course and sometimes decreases below the steady dark current during the decay course.[13]

Salis *et al.* have presented a simple kinetic model for PPC by means of a set of rate equations.[14] Unfortunately, it has not been verified by any experimental results so far and needs to be further optimized. In this work, we have refined and verified the model with experimental data. The very closely matched numerical solutions support the correctness of this model. In addition, we have predicted the densities of trapped holes, electrons, and electrons in the conduction band during the PPC. So an experimentally verified model could be built to predict the behaviors of PPC and NPC in GaN HEMTs.

Samples used in this work are procured from Nanjing Electronic Devices Institute, China. This device was grown on a 450 μm thick sapphire substrate. It consists of a 2 μm GaN channel layer and a 22 nm AlGaN barrier layer. Ni/Au is used as a Schottky contact, and SiN is used as a passivation layer. The source-to-gate spacing, gate-to-drain spacing, and gate length are 0.8, 2.7, and 0.35 μm, respectively. The sample is composed of 10 fingers, and the total gate width is 1.25 mm.

First, it is important to determine the steady states with and without illumination. Figure 1 shows the experimental results concerning trapping and detrapping/recovery transients with and without illumination. Due to the same measuring bias, current levels are only affected by the illumination condition. This means that the trapped electrons during the filling pulse will be released to a certain density under the same measuring bias and illumination condition. So, in the situation that the current level has not reached the steady state, a compensation could be used to predict the final current level, which will be
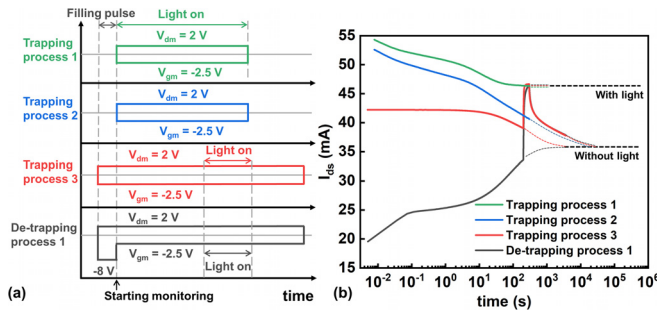
FIG. 1. (a) Sequence of biases including two trapping transients and two detrapping transients. Green, blue, and red are the trapping transients. Notice that the filling pulse in the red one had the same bias as the measuring process. Black is a detrapping transient including a 10-s-long filling pulse with a V_{gm} value of -8 V and a measuring process. (b) Current transients with two steady-state current levels.

employed in our following model. In addition, Fig. 1(b) provides a fast way to acquire the steady state in a detrapping transient by measuring the trapping process with the same bias to identify the upper limit, that is, the clamping method, which can be used to judge if there is a detrapping behavior with a long time constant beyond the measuring window.

Two kinds of defects acting as electron and hole traps have been considered in the model. For the electron traps that can capture charges from the conduction band, their steady-state density of trapped electrons under the excitation is decided by the Arrhenius probability of releasing and the probability of capturing. Here, we only consider electron traps that contribute to the channel current, whose energy level can be calculated from detrapping transients at various temperatures.[12] When the exciting light starts, a great number of electron-hole pairs will generate in centers. Electrons are injected into the conduction band, while holes are trapped in centers. For those in the AlGaN or GaN bulk, photogenerated electrons could be found partly in the conduction band and then will be driven to the quantum well by the vertically oriented field or the built-in electric field associated with the band bending at the interface and partly returning centers due to an electron-hole recombination. This build-up course of PPC could be described as follows:

$$\frac{dm}{dt} = \Phi\sigma_e(M_T - m) - R_e n_c m, \tag{1}$$

$$\frac{dn}{dt} = n_c C_e(N_T - n) - \sum_{i=1}^{n} s_i e^{\left(-\frac{E_i}{kT}\right)} n, \tag{2}$$

$$\frac{dn_c}{dt} = \Phi\sigma_e(M_T - m) - R_e n_c m - n_c C_e(N_T - n) + \sum_{i=1}^{n} s_i e^{\left(-\frac{E_i}{kT}\right)} n, \tag{3}$$

where m, n, and n_c (centimeter per cubic meter) are the densities of trapped holes, electrons, and electrons in the conduction band, respectively, Φ (per square centimeter per second) is the flux of exciting photons, σ_e (centimeter square) is the cross section of electron-hole pair photoproduction, M_T and N_T (centimeter per cubic meter) are the densities of electron and hole traps, respectively, C_e and R_e (per square centimeter per second) are the possibilities of electron capture by traps and electron-hole recombination, respectively, s_i (per second) and E_i (electron volt) are the frequency factor and energy level of the ith

detrapping behavior, respectively, k is the Boltzmann constant, and T (Kelvin) is the temperature of the active region as shown in Fig. 2.

Before the calculations of the model, the above equations have been normalized by substituting $x = n/M_T$, $y = m/M_T$, $z = n_c/M_T$, $\widetilde{C}_e = C_e M_T$, and $\widetilde{R}_e = R_e M_T$,

$$\frac{dy}{dt} = \Phi\sigma_e(1 - y) - \widetilde{R}_e zy, \tag{4}$$

$$\frac{dx}{dt} = \widetilde{C}_e z(N_T/M_T - x) - \sum_{i=1}^{n} s_i e^{\left(-\frac{E_i}{kT}\right)} x, \tag{5}$$

$$\frac{dz}{dt} = \Phi\sigma_e(1 - y) - \widetilde{R}_e zy - \widetilde{C}_e z(N_T/M_T - x) + \sum_{i=1}^{n} s_i e^{\left(-\frac{E_i}{kT}\right)} x. \tag{6}$$

The decay course of PPC could be expressed by substituting $\Phi\sigma_e = 0$. In addition, the initial state of the above rate equations is assumed to be steady right before lighting on. However, it is rather a long time ($>10^3$ s) to acquire such a state for many devices as well as ours. During the build-up course, the strongly exciting light is the primary factor that affects the electron density in the conduction band, temporarily suppressing the trapping or detrapping behavior that has not fully captured or released electrons to the steady-state density. So an exponential correction, that is, $A[1 - \exp(-t/\tau)]$, has been considered in this model[12] to compensate the decay course of PPC, where A stands for the amplitude and τ stands for the trap's time constant. Here, we used $[1 - \exp(-t/\tau)]$ rather than $\exp(-t/\tau)$ due to the fact that the detrapping transients were employed in our experiments.

Now, we can obtain the normalized electron density of the conduction band in the decay course as follows:

$$\frac{dz}{dt} = -\widetilde{R}_e zy - \widetilde{C}_e z(N_T/M_T - x) + \sum_{i=1}^{n} s_i e^{\left(-\frac{E_i}{kT}\right)} x + A(1 - e^{(-t/\tau)}). \tag{7}$$
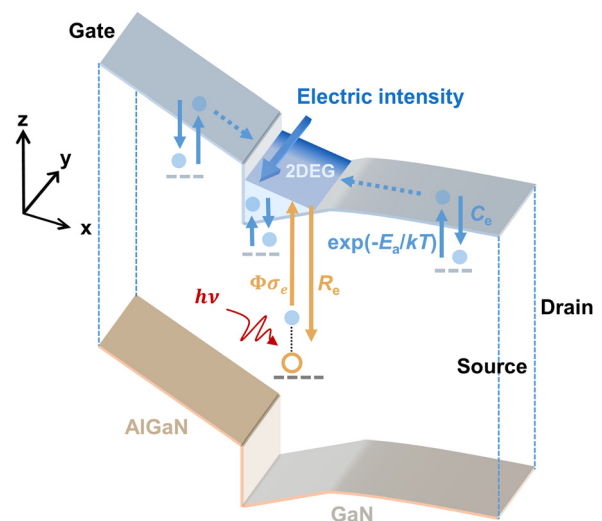

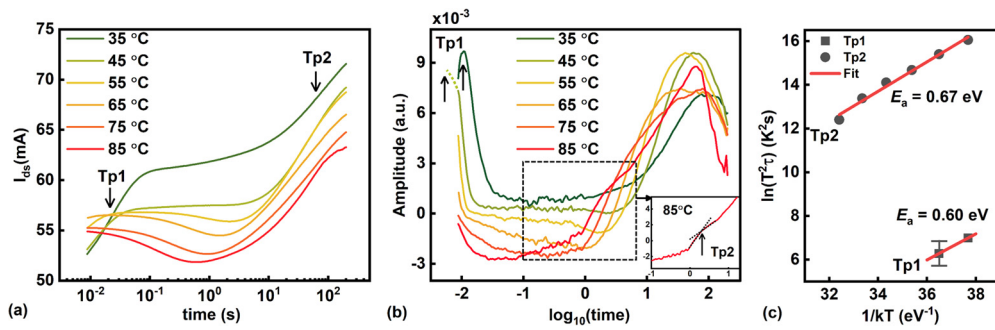**FIG. 2.** Simplified level scheme for the build-up course of PPC.

FIG. 3. (a) Detrapping transients at various temperatures with 10-s-long filling biases of $V_{df} = 10$ V and $V_{gf} = -2$ V. Two detrapping behaviors contributed to the channel current named Tp1 and Tp2, respectively. (b) The corresponding time constant spectra of Tp1 and Tp2 at various temperatures. Note that the time constants of Tp1 were beyond the measuring window at the temperature higher than 45 °C, but the thermal level could be estimated according to the trend of the time constant spectra. (Inset) The time constant of Tp2 at 85 °C. Its temperature dependence could be used to extract the Arrhenius plots. (c) Extracted Arrhenius plots of Tp1 and Tp2 with the thermal energy levels of 0.60 and 0.67 eV, respectively.

The thermal depth of electron traps, which contributes to the channel current within the measuring window, could be extracted from the Arrhenius plots at various temperatures.[12] Figure 3 shows the detrapping transients, corresponding time constant spectra,[15] and Arrhenius plots. Notice that the time constant of Tp2 is shown in the inset of Fig. 3(b). An off-state trap-filling bias of $V_{gs} = -10$ V and $V_{ds} = 2$ V was applied to the sample[16] using an Agilent B1500A, and then a measuring bias of $V_{gs} = -2$ V and $V_{ds} = 2$ V was used to monitor the detrapping process. Experiments were repeated at temperatures

from 35 °C to 85 °C. The corresponding time constant spectra were calculated from the current transients using $\partial I_{ds}/\partial \log_{10}(t)$ as shown in Fig. 3(b). Because the PPC measurements were carried out at 35 °C, only the detrapping behaviors affecting the current level at 35 °C, that is, Tp1 and Tp2 with energy levels of 0.60 and 0.67 eV, respectively, were considered in the model. In particular, traps with the same energy level have been identified in Refs. 17–19, which have been identified at the AlGaN/GaN interface or in the GaN buffer layer.
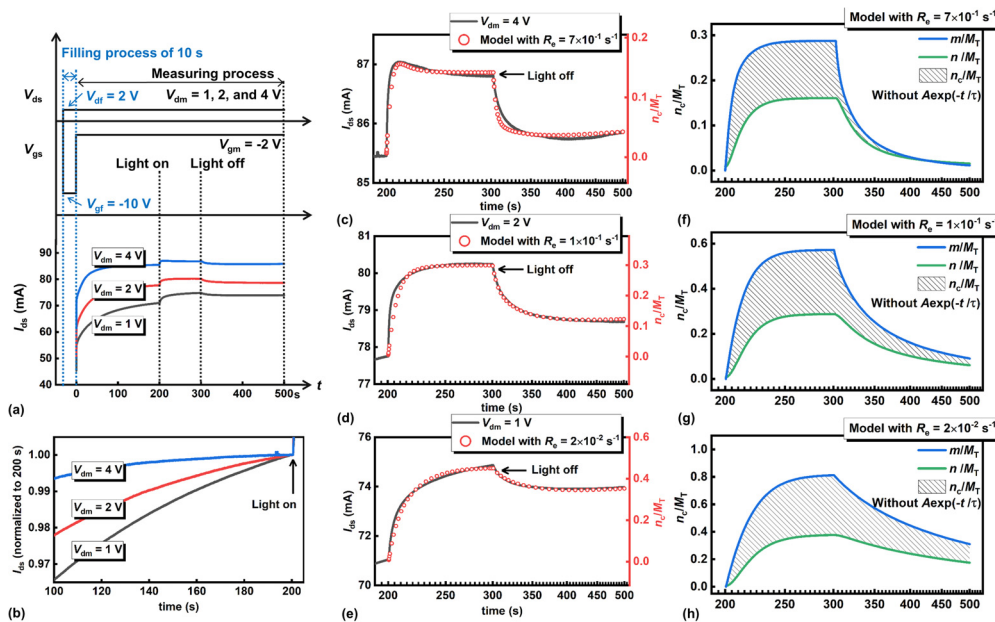

FIG. 4. (a) Sequence of experiments with the measuring voltage of 1, 2, and 4 V. The filling pulse is 10 s with the same bias of $V_{gf} = -10$ V and $V_{df} = 2$ V. The light was switched on at 200 s and off at 300 s. Experiments were carried out at 35 °C. (b) Normalized current transients from 100 s to 210 s. The higher the measuring voltage is, the closer the detrapping behaviors are to the steady state. (c) Experimental data with the V_{dm} value of 4 V and model with the $\widetilde{R}_e$ and A values of 7×10^{-1} s^{-1} and 0.05, respectively. Note that there is a NPC in the build-up course and also predicted by the model with $\widetilde{R}_e \gg \widetilde{C}_e$. (d) Experimental data with the V_{dm} value of 2 V and model with the $\widetilde{R}_e$ and A values of 1×10^{-1} s^{-1} and 0.125, respectively. (e) Experimental data with the V_{dm} value of 1 V and model with the $\widetilde{R}_e$ and A values of 2×10^{-2} s^{-1} and 0.32, respectively. (f) Densities of trapped holes, electrons, and electrons in the conduction band with $\widetilde{R}_e \gg \widetilde{C}_e$. (g) Densities of trapped holes, electrons, and electrons in the conduction band with $\widetilde{R}_e \approx \widetilde{C}_e$. (h) Densities of trapped holes, electrons, and electrons in the conduction band with $\widetilde{R}_e \ll \widetilde{C}_e$. Notice that a logarithm time scale is employed in (c)–(h).

The measured value of the energy flux of exciting light (Φ) was 19.5 mW/cm^2, and a photon flux of 3.93×10^{16} cm^{-2} s^{-1} could be calculated according to the 400 nm light. The cross section σ_e was chosen to be 10^{-18} cm^{-2}.[20] As a result, a $\Phi\sigma_e$ value of 4×10^{-2} s^{-1} was used in the model. N_T/M_T was placed equal to 1. For the rest of the parameters, their exact values were chosen to suit the measured experimental results. $\widetilde{C}_e$ was chosen to be 8×10^{-2} s^{-1}. s_1 and s_2, which correspond to the trap with thermal depths of 0.60 and 0.67 eV, were chosen to match their contributions to the channel current, that is, 1×10^8 and 8×10^9 s^{-1},[21] respectively. Now, only $\widetilde{R}_e$ has been waiting for the assignment.

Figure 4(a) shows the measuring sequence of three curves at 35 °C with the V_{dm} values of 1, 2, and 4 V, respectively. These three situations had different electrical field distributions in the device. A higher V_{dm} value leads to a higher electric field along the channel. Notice that the value of 4 V has already reached the saturated region at a gate bias of −2 V. As a result, a generation of hot electrons with higher average energy could be expected, which has a larger probability of recombination, that is, $\widetilde{R}_e$.

Interestingly, this model has predicted a situation that when $\widetilde{R}_e \gg \widetilde{C}_e$, a nonmonotonous build-up course may happen.[14] This phenomenon has been observed in Fig. 4(c) with $\widetilde{R}_e$ and $\widetilde{C}_e$ of 7×10^{-1} s^{-1} and 8×10^{-2} s^{-1}, respectively, which cannot be explained by the stretched exponentials, supporting the correctness of this model. Only $\widetilde{R}_e$ was changed in Figs. 4(c), 4(d), and 4(e) to match the measured curves. Figures 4(f), 4(g), and 4(h) show the corresponding densities of trapped holes and electrons. In addition, a part of trapped electrons in the filling process has not been completely released as shown in Fig. 4(b). The lower the V_{dm}, the more the electrons were waiting to be released. As we mentioned before, a detrapping behavior of $A\,[1 - \exp(-t/\tau)]$[19] has been considered to correct the PPC decay with a τ value of 200 s and A values of 0.05, 0.125, and 0.32.

We have enriched a kinetic model for PPC and verified it using experimental data. Based on the physical nature, this model derives a formula that fits the actual situation well. The NPC could happen when $\widetilde{R}_e \gg \widetilde{C}_e$, which cannot be explained using a traditional stretched exponential function. This work provides an experimentally verified model with clear and meaningful parameters. We hope that this model can contribute to the further understanding of PPC in GaN HEMTs.

REFERENCES

[1] H. Amano, Y. Baines, E. Beam, M. Borga, T. Bouchet, P. R. Chalker, M. Charles, K. J. Chen, N. Chowdhury, R. Chu, C. De Santi, M. Merlyne De Souza, S. Decoutere, L. Di Cioccio, B. Eckardt, T. Egawa, P. Fay, J. J. Freedsman, L. Guido, O. Häberlen, G. Haynes, T. Heckel, D. Hemakumara, P. Houston, J. Hu, M. Hua, Q. Huang, A. Huang, S. Jiang, H. Kawai, D. Kinzer, M. Kuball, A. Kumar, K. Boon Lee, X. Li, D. Marcon, M. März, R. McCarthy, G. Meneghesso, M. Meneghini, E. Morvan, A. Nakajima, E. M. S. Narayanan, S. Oliver, T. Palacios, D. Piedra, M. Plissonnier, R. Reddy, M. Sun, I. Thayne, A. Torres, N. Trivellin, V. Unni, M. J. Uren, M. Van Hove, D. J. Wallis, J. Wang, J. Xie, S. Yagi, S. Yang, C. Youtsey, R. Yu, E. Zanoni, S. Zeltner, and Y. Zhang, J. Phys. D: Appl. Phys. **51**, 163001 (2018).

[2] W. Zhang, J. Xue, L. Zhang, T. Zhang, Z. Lin, J. F. Zhang, and Y. Hao, Appl. Phys. Lett. **110**, 252102 (2017).

[3] W. Sun, J. Joh, S. Krishnan, S. Pendharkar, C. M. Jackson, S. A. Ringel, and A. R. Arehart, IEEE Trans. Electron Devices **66**, 890–895 (2019).

[4] Y. Huang, D. J. Chen, H. Lu, H. B. Shi, P. Han, R. Zhang, and Y. D. Zheng, Appl. Phys. Lett. **96**, 243503 (2010).

[5] J. H. Lee, W. W. Lee, D. W. Yang, W. J. Chang, S. S. Kwon, and W. I. Park, ACS Appl. Mater. Interfaces **10**, 14170–14174 (2018).

[6] B. Ozden, M. P. Khanal, V. Mirkhani, K. Yapabandara, C. Yang, S. Ko, S. Youn, M. C. Hamilton, M. H. Sk, A. C. Ahyi, and M. Park, J. Nanosci. Nanotechnol. **16**, 7630–7634 (2016).

[7] G. Beadie, W. S. Rabinovich, A. E. Wichenden, D. D. Koleske, S. C. Binari, and J. A. Freitas, Appl. Phys. Lett. **77**, 1092–1094 (1997).

[8] B. K. Li, W. K. Ge, J. N. Wang, and K. J. Chen, Appl. Phys. Lett. **92**, 082105 (2008).

[9] H. Chen, R. Chen, N. K. Rajan, F. Chang, L. Chen, K. Chen, Y. Yang, and M. A. Reed, Phys. Rev. B **84**, 205443 (2011).

[10] X. Tang, B. Li, H. A. Moghadam, P. Tanner, J. Han, H. Li, S. Dimitrijev, and J. Wang, Jpn. J. Appl. Phys. **57**, 175105 (2018).

[11] O. Mitrofanov and M. Manfra, Superlattices Microstruct. **34**, 33–53 (2003).

[12] J. Joh and J. A. del Alamo, IEEE Trans. Electron Devices **58**, 132–140 (2011).

[13] X. Tang, B. Li, K. J. Chen, and J. Wang, Appl. Phys. Express **11**, 054101 (2018).

[14] M. Salis, A. Anedda, F. Quarati, A. J. Blue, and W. Cunningham, J. Appl. Phys. **97**, 033709 (2005).

[15] M. Tapajna, R. J. T. Simms, Y. Pei, U. K. Mishra, and M. Kuball, IEEE Electron Device Lett. **31**, 662–664 (2010).

[16] P. A. Butler, M. Uren, B. Lambert, and M. Kuball, IEEE Trans. Nucl. Sci. **65**, 2862–2869 (2018).

[17] X. Zheng, S. Feng, Y. Zhang, X. He, and Y. Wang, IEEE Trans. Electron Devices **64**, 1498–1504 (2017).

[18] D. Bisi, M. Meneghini, C. de Santi, A. Chini, M. Dammann, P. Brückner, M. Mikulla, G. Meneghesso, and E. Zanoni, IEEE Trans. Electron Devices **60**, 3166–3175 (2013).

[19] X. Zheng, S. Feng, Y. Zhang, and J. Yang, Microelectron. Reliab. **63**, 46–51 (2016).

[20] R. Passler, J. Appl. Phys. **96**, 715–722 (2004).

[21] R. Chen R and S. W. S. Mckeever, *Theory of Thermoluminescence and Related Phenomena* (World Scientific, Singapore, 1997).